HHS Public Access

Author manuscript

J Thromb Haemost. Author manuscript; available in PMC 2016 January 01.

Published in final edited form as:

J Thromb Haemost. 2015 January ; 13(1): 57–71. doi:10.1111/jth.12770.

Coagulation-driven platelet activation reduces cholestatic liver injury and fibrosis in mice

N. Joshi[*,‡], **A. K. Kopec**[†], **K. M. O'Brien**[*,‡], **K. L. Towery**[†], **H. Cline-Fedewa**[†], **K.J. Williams**[†], **B. L. Copple**[*,‡], **M. J. Flick**[§], and **J. P. Luyendyk**[†,‡,1]

[*]Department of Pharmacology & Toxicology, Michigan State University, East Lansing, Michigan 48824

[†]Department of Pathobiology & Diagnostic Investigation, Michigan State University, East Lansing, Michigan 48824

[‡]Center for Integrative Toxicology, Michigan State University, East Lansing, Michigan 48824

[§]Division of Experimental Hematology and Cancer Biology, Cincinnati Children's Hospital Medical Center, Cincinnati, Ohio 45229

Summary

Background—The coagulation cascade has been shown to participate in chronic liver injury and fibrosis, but the contribution of various thrombin targets, such as protease activated receptors (PARs) and fibrin(ogen), has not been fully described. Emerging evidence suggests that in some experimental settings of chronic liver injury, platelets can promote liver repair and inhibit liver fibrosis. However, the precise mechanisms linking coagulation and platelet function to hepatic tissue changes following injury remain poorly defined.

Objectives—To determine the role of PAR-4, a key thrombin receptor on mouse platelets, and fibrin(ogen) engagement of the platelet $\alpha_{IIb}\beta_3$ integrin in a model of cholestatic liver injury and fibrosis.

Methods—Biliary and hepatic injury was characterized following 4 week administration of the bile duct toxicant α-naphthylisothiocyanate (ANIT) (0.025%) in PAR-4-deficient mice (PAR-4$^{-/-}$

[1]To whom correspondence should be addressed: James P. Luyendyk, Department of Pathobiology and Diagnostic Investigation, Michigan State University, 1129 Farm Lane, 253 Food Safety and Toxicology Building, East Lansing, MI 48824, Phone: (517) 884-2057, luyendyk@cvm.msu.edu.

Author contributions:

Participated in concept and research design: N. Joshi, A. K. Kopec, M. J. Flick, J. P. Luyendyk

Conducted experiments: A. K. Kopec, N. Joshi, K. M. O'Brien, K. L. Towery, H. Cline-Fedewa, M. J. Flick, J. P. Luyendyk

Performed data analysis and interpreted data: N. Joshi, K. J. Williams, J. P. Luyendyk

Wrote or contributed to the writing of the manuscript: N. Joshi, A. K. Kopec, K. M. O'Brien, K. L. Towery, K. J. Williams, B. L. Copple, M. J. Flick, J. P. Luyendyk

Final approval of the version to be published: N. Joshi, A. K. Kopec, K. M. O'Brien, K. L. Towery, H. Cline-Fedewa, K. Williams, B. L. Copple, M. J. Flick, J. P. Luyendyk

Disclosure:

H. Cline-Fedewa, A. K. Kopec, B. L. Copple, K. M. O'Brien, K. J. Williams, K. L. Towery and N. Joshi report grants from National Institutes of Health during the conduct of the study.

J. P. Luyendyk reports grants from National Institutes of Health during the conduct of the study and grants from Boehringer Ingelheim and Conatus Pharmaceuticals outside the submitted work.

M. J. Flick has nothing to disclose.

mice), mice expressing a mutant form of fibrin(ogen) incapable of binding integrin $\alpha_{IIb}\beta_3$ (Fib$\gamma^{\Delta 5}$), and wild-type mice.

Results—Elevated plasma thrombin-antithrombin and serotonin levels, hepatic fibrin deposition and platelet accumulation in liver accompanied hepatocellular injury and fibrosis in ANIT-treated wild-type mice. PAR-4 deficiency reduced plasma serotonin levels, increased serum bile acid concentration, and exacerbated ANIT-induced hepatocellular injury and peribiliary fibrosis. Compared to PAR-4-deficient mice, ANIT-treated Fib$\gamma^{\Delta 5}$ mice displayed more widespread hepatocellular necrosis accompanied by marked inflammation, robust fibroblast activation and extensive liver fibrosis.

Conclusions—Collectively, the results indicate that PAR-4 and fibrin-$\alpha_{IIb}\beta_3$ integrin engagement, pathways coupling coagulation to platelet activation, each exert hepatoprotective effects during chronic cholestasis.

Keywords

Blood coagulation; Platelets; Fibrin; Liver disease; Fibrosis

Introduction

Coagulation cascade activation, marked by thrombin generation, hepatic fibrin deposition, and platelet activation is a conspicuous feature of cholestatic liver disease in humans [1–3], which is recapitulated in experimental settings of chronic liver injury [2, 4]. Experimental evidence supports a role for protease activated receptors (PARs), including the thrombin receptor PAR-1, in promoting liver fibrosis [5, 6]. PAR-1 deficiency reduced hepatic collagen deposition in models of carbon tetrachloride, bile duct ligation (BDL) and alpha-naphthylisothiocyanate (ANIT)-induced liver fibrosis [2, 4, 7, 8], an observation likely connected to PAR-1 expression by macrophages and/or hepatic stellate cells [4, 8, 9]. Unlike humans, PAR-1 is not expressed by mouse platelets, and thrombin-mediated platelet activation is intact in PAR-1-deficient mice [10]. A complex of PAR-3 and PAR-4 contributes to thrombin-mediated platelet activation in mice [11, 12]. Thus, while PAR-1$^{-/-}$ mice have provided compelling evidence of profibrogenic effects of thrombin, these cannot be attributed to platelet activation.

Indeed, the mechanisms coupling thrombin activity to platelet activation in models of liver fibrosis have not been fully explored. It is conceivable that thrombin, through activation of PAR-1 (in humans) or PAR-3/4 (in mice), is central to platelet activation in liver disease. Thrombin is a very potent activator of platelets, causing degranulation and release of stored mediators, including serotonin [13]. Platelet activation by diverse mediators, including thrombin, alters the conformation of integrin $\alpha_{IIb}\beta_3$, revealing a high affinity binding site for fibrin(ogen) [14]. Fibrin(ogen) engagement of activated $\alpha_{IIb}\beta_3$ integrin can further modify platelet activation, being critical for platelet aggregation and clot retraction [14, 15]. Demonstrating the importance of this interaction, mice expressing a mutant fibrin(ogen) incapable of binding activated $\alpha_{IIb}\beta_3$ integrin have defective platelet aggregation, despite retention of other fibrin(ogen)-dependent hemostatic functions [15]. However, the role of

this functional interaction between platelets and fibrin(ogen) in chronic liver injury has not yet been defined.

The contribution of platelets in experimental settings of liver damage and fibrosis appears to be context-dependent. Studies suggest that platelets can either promote or reduce liver injury and fibrosis. The specific role of platelets depends on the etiology of the liver disease or nature of the hepatic injury [16]. Moreover, experimental variables including the degree and duration of platelet deficiency or inhibition also impacts the outcome with respect to liver injury and fibrosis [17, 18]. For example, platelets exacerbate acute cholestatic liver injury in multiple models [19–21], whereas long-term thrombocytopenia or serotonin deficiency exacerbates liver fibrosis [17, 22]. Coagulation-mediated platelet activation, through both thrombin- and fibrin(ogen)-mediated mechanisms, is central to normal hemostasis [23]. However, the impact of these platelet activation pathways on chronic cholestatic liver injury has not yet been specifically evaluated.

In the present study, we sought to identify key mechanisms that link platelet function to liver injury and fibrosis in an experimental setting of chronic bile duct injury. Utilizing PAR-4 deficient mice (PAR-4$^{-/-}$) and mice expressing a mutant form of fibrin(ogen) lacking the binding motif for integrin $\alpha_{IIb}\beta_3$ (Fib$\gamma^{\Delta 5}$) [15, 24], we determined the role of thrombin-mediated platelet activation and fibrin(ogen)-platelet interactions through the integrin $\alpha_{IIb}\beta_3$ in chronic biliary injury and fibrosis.

Materials and Methods

Mice

PAR-4$^{-/-}$ mice, Fib$\gamma^{\Delta 5}$ mice, and wild-type mice backcrossed at least 8 generations on the same C57Bl/6J background, were maintained by homozygous breeding [15, 24]. Age-matched male mice between the ages of 8–14 weeks were used for these studies. Mice were housed at an ambient temperature of approximately 22°C with alternating 12 hour light/12 hour dark cycles and provided purified water and rodent chow *ad libitum* prior to study initiation. Mice were maintained in Association for Assessment and Accreditation of Laboratory Animal Care International-accredited facilities at Michigan State University or Cincinnati Children's Hospital Medical Center. All animal procedures were approved by Michigan State University or Cincinnati Children's Hospital Medical Center Institutional Animal Care and Use Committees.

ANIT diet model

Custom diets were prepared by Dyets, Inc. (Bethlehem, PA). The ANIT diet was an AIN-93M diet containing 0.025% ANIT (Sigma-Aldrich, St. Louis, MO). The control diet was AIN-93M diet. Groups of mice were fed each diet for a total of 4 weeks, *ad libitum*. Mice fed ANIT diet are referred to as ANIT-treated mice. Mice were anesthetized with isoflurane, and blood was collected from the caudal vena cava into sodium citrate (final, 0.38%) or an empty syringe for the collection of plasma and serum, respectively. The liver was removed and washed with saline. The left medial lobe of the liver was affixed to cork with optimal cutting temperature compound (VWR Scientific, Radnor, PA) and frozen for 3

minutes in liquid nitrogen-chilled isopentane. Sections of the left lateral lobe were fixed in neutral-buffered formalin for 48 hours prior to routine processing. The remaining liver was cut into approximately 100 mg sections and flash-frozen in liquid nitrogen.

Histopathology and clinical chemistry

For analysis of liver histopathology by light microscopy, formalin-fixed liver sections were cut at 5 microns and stained with hematoxylin and eosin (H&E) and sirius red by the Michigan State University Investigative Histopathology Laboratory. At least 2 sections of liver from the left lateral lobe of each animal were qualitatively evaluated in their entirety by a Board-certified veterinary pathologist (K.J.W.). Quantitative measures of necrosis (i.e., lesion frequency and size) in H&E-stained sections were performed in a masked fashion using ImageJ. For quantification of Sirius red staining (collagen deposits), images of Sirius-red stained liver sections were captured using a Virtual Slide System VS110 (Olympus, Hicksville, NY) with a 20X objective. Random images were derived from the digitized slides approximating at least 100 mm^2 tissue for each liver. The area of positive sirius red staining in each image was determined in an unbiased fashion using a batch macro and the color deconvolution tool in ImageJ. Total bile acids in serum were determined using a colorimetric assay (Bio-Quant, San Diego, CA) and serum activities of alanine aminotransferase (ALT) and alkaline phosphatase (ALP) were determined using commercial reagents (Thermo Scientific, Waltham, MA; Pointe Scientific, Canton, MI). Plasma thrombin-antithrombin (TAT) and serotonin levels were determined using commercial enzyme-linked immunosorbent assay kits (Siemens Healthcare Diagnostics, Deerfield, IL; Eagle Biosciences, Nashua, NH). Serum cytokine levels (IL-6, IL-4, KC/Gro, TNFα) were determined using the Meso Scale V-PLEX Proinflammatory Panel Kit and a Sector 600 Imager (Meso Scale Discovery, Rockville, MD).

Immunohistochemistry and immunofluorescence

α-smooth muscle actin (α-SMA) immunohistochemistry was performed as described previously [25], with slight modification. Briefly, sections were de-paraffinized in xylene and subjected to heat-mediated antigen retrieval in citrate buffer (10 mM, pH 6). Sections were incubated with primary rabbit-anti α-SMA antibody (1:750) (Abcam, Cambridge, MA). Fibrin(ogen) immunohistochemistry was performed on de-paraffinized formalin-fixed sections after antigen retrieval with proteinase K, using a rabbit anti-human fibrin(ogen) antibody (1:600) (Dako North America, Carpinteria, CA). Each primary antibody was detected utilizing a biotinylated goat anti-rabbit antibody (Jackson ImmunoResearch Laboratories, West Grove, PA) and Vectastain Elite ABC kit and ImmPACT DAB substrate (Vector Laboratories, Burlingame, CA). Immunofluorescent staining of type 1 collagen, cytokeratin-19 (CK19) and integrin α_{IIb}/CD41 (platelet) were performed as described [2, 20, 26]. Prolong Gold (DAPI-containing) Antifade reagent (Life Technologies) was applied to the tissues prior to cover slipping. Fluorescent staining in liver sections was visualized using an Olympus DP70 microscope (Olympus, Lake Success, NY) and merged (as appropriate) using Olympus DP Manager software. Type 1 collagen and CK19 staining was quantified using Scion Image (Scion Corporation, Frederick, MD) as described previously [2], utilizing approximately 10 low-power images (100X) for each tissue. The percentage of pixels containing positive signal (i.e., collagen staining) was expressed as a fold change relative to

wild-type mice fed control diet. Neutrophil and CD3 staining on paraffin-embedded, formalin-fixed sections was accomplished using monoclonal rat anti-mouse allotypic neutrophil marker (PMN 7/4) and rabbit polyclonal anti-CD3 (Abcam), respectively, and was performed by the Michigan State University Investigative Histopathology Laboratory. Quantification of α-SMA and CD3 positive staining was performed using digitized slides and ImageJ as described for Sirius red staining (above).

RNA isolation, cDNA synthesis, and real-time PCR

Total RNA was isolated from approximately 15 mg of snap-frozen liver using TRI Reagent (Molecular Research Center, Cincinnati, OH). 1 μg of total RNA was utilized for the synthesis of cDNA, accomplished using a High-Capacity cDNA Reverse Transcription kit (Applied Biosystems, Foster City, CA) and a C1000 Thermal Cycler (Bio-Rad Laboratories, Hercules, CA). Hepatic levels of mRNAs encoding the profibrogenic genes type 1 collagen (COL1A1), integrin β6 (ITGB6), transforming growth factor-1 (TGFβ1) and -2 (TGFβ2) and tissue inhibitor of metalloproteinase1 (TIMP-1) were determined using SYBR Green PCR, iTaq (Bio-Rad), and a CFX Connect thermal cycler (Bio-Rad). Primers were purchased from IDT (Coralville, IA). The expression of each gene was adjusted to the geometric mean Ct of two individual housekeeper genes, HPRT and 18S RNA, as described [27], and the relative levels of each gene were evaluated using the ΔΔCt method. Sequences for primers used are available in supplemental data.

Platelet isolation and stimulation

Approximately 0.5 mL whole blood was collected from the caudal vena cava into acid citrate dextrose (ACD) and added to an equivalent volume of pipes saline glucose (PSG). Platelet-rich plasma was mixed with PSG containing 1 μM PGE_1 and 0.02U/ml apyrase and subjected to centrifugation at 500 × g for 10 min. Platelets were then subjected to one additional wash with PSG+ PGE_1/apyrase and then gently resuspended in DMEM at a density of approximately 1×10^8 platelets/100μL. The platelets were then stimulated with thrombin (10 U/ml) or its vehicle (PBS) for 5 minutes and after centrifugation, 0.1% ascorbic acid added to the supernatant to stabilize serotonin. Supernatant serotonin levels were determined using a commercial ELISA (Eagle Biosciences).

Statistics

Comparison of two groups was performed using Student's t-test. Comparison of three or more groups was performed using one- or two-way analysis of variance (ANOVA), as appropriate, and Student-Newman-Keul's *post hoc* test. The criterion for statistical significance was $p \leq 0.05$.

Results

Increased coagulation and platelet accumulation in livers of wild-type mice

Compared to wild-type mice fed control diet, plasma TAT levels were increased in ANIT-treated mice, indicating activation of the coagulation cascade (Fig. 1A). Platelets are the primary cellular source of peripheral serotonin, a mediator shown to exert hepatoprotective effects in liver fibrosis [22, 28]. Plasma levels of serotonin were increased in ANIT-treated

mice (Fig. 1B). Minimal fibrin deposition was observed in wild-type mice fed control diet (Fig. 1C). In contrast, an increase in peribiliary and sinusoidal fibrin deposits was evident in ANIT-treated mice (Fig. 1C). Fibrin was also apparent in association with focal areas of hepatocellular necrosis, although these lesions were infrequent in wild-type mice (Fig. 1C). Scattered α_{IIB} (platelet) staining was confined to sinusoids and larger vessels in mice fed control diet. Hepatic platelet accumulation was evident in livers of ANIT-treated mice (Fig. 1D). Taken together, the results indicate that ANIT toxicity in mice is associated with activation of the coagulation cascade, hepatic fibrin deposition and platelet accumulation and activation.

Effect of PAR-4 deficiency on serotonin levels, liver injury and biliary hyperplasia in ANIT-treated mice

Plasma TAT levels were similar in ANIT-treated wild-type mice (3.8 ± 1.2 ng/ml, n=10) and ANIT-treated PAR-4$^{-/-}$ mice (3.2 ± 0.5 ng/ml, n=12). Thrombin stimulation has been shown to induce the rapid release of serotonin from human platelets [13]. Consistent with this, we found that thrombin stimulation induced serotonin release from isolated wild-type platelets, and this was significantly reduced in isolated PAR-4$^{-/-}$ platelets (Supplemental Fig. 1). Plasma serotonin levels increased in ANIT-treated wild-type mice, but not in ANIT-treated PAR-4$^{-/-}$ mice (Fig. 2A). A previous study suggested that platelet-derived serotonin inhibits cholestatic liver injury, in part through regulation of the bile acid pool [22]. Consistent with this observation, serum bile acids increased significantly in ANIT-treated wild-type mice, and increased further in ANIT-treated PAR-4$^{-/-}$ mice (Fig. 2B). Serum ALT and ALP activities increased to a greater extent in ANIT-treated PAR-4$^{-/-}$ mice compared to ANIT-treated wild-type mice (Fig. 2C–D). The overall histological appearance of control diet fed WT and PAR4$^{-/-}$ mice was similar (Fig. 2F). In agreement with the increase in serum ALT, the number of necrotic lesions was significantly increased in livers of ANIT-treated PAR-4$^{-/-}$ mice compared to ANIT-treated wild-type mice, although the average size of necrotic foci was unaffected by genotype (Fig. 2E).

ANIT-treated mice developed biliary hyperplasia, which was not affected by genotype, as indicated by CK19 staining and quantification (Supplemental Fig. 2A–B). Liver histopathology indicated increased portal inflammation and biliary fibrosis in ANIT-treated wild-type mice (Fig. 2F), which qualitative assessment suggested was slightly more severe in PAR-4$^{-/-}$ mice. In agreement with previous studies [26, 29, 30], we identified portal inflammation in ANIT-treated mice as predominantly a lymphocytic infiltrate. Indeed, accumulation of CD3^{+} lymphocytes increased in ANIT-treated wild-type mice, and this was exacerbated in ANIT-treated PAR-4$^{-/-}$ mice (Supplemental Fig. 3A–B). Consistent with enhanced inflammation, plasma IL-6 levels were significantly increased in ANIT-treated PAR-4$^{-/-}$ mice, although other cytokines examined were unaffected (Supplemental Fig. 3C).

Increased liver fibrosis in ANIT-treated PAR-4$^{-/-}$ mice

Because our analysis of liver histopathology suggested more peribiliary fibrosis in PAR-4$^{-/-}$ mice, we examined the expression of profibrogenic changes and collagen deposits in ANIT-treated mice. Hepatic expression of profibrogenic COL1A1, TGFβ2, ITGB6, and TIMP-1

mRNAs was increased significantly in livers of ANIT-treated wild-type mice compared to control diet fed animals (Fig. 3A). Induction of each mRNA increased further in ANIT-treated PAR-4$^{-/-}$ mice, although increases in TGFβ1 and TGFβ2 mRNA did not achieve statistical significance (Fig. 3A). Peribiliary expression of α-SMA, a marker of activated hepatic stellate cells and portal fibroblasts, increased in livers of ANIT-treated wild-type mice (Fig. 3B), and this increase was larger in livers of ANIT-treated PAR-4$^{-/-}$ mice (Fig. 3B–C). Peribiliary collagen deposition, as indicated by sirius red staining (Fig 4A–B) and type 1 collagen immunofluorescence (Fig. 4C–D), increased in livers of ANIT-treated wild-type mice compared to control diet fed wild-type mice. In agreement with liver histology and profibrogenic gene expression, this was significantly increased in livers of ANIT-treated PAR-4$^{-/-}$ mice (Fig. 4B and 4D).

Increased hepatocellular necrosis and hepatic inflammation in ANIT-treated Fib$\gamma^{\Delta 5}$ mice

Fib$\gamma^{\Delta 5}$ mice express normal levels of a mutant fibrin(ogen) that does not bind to the platelet integrin $\alpha_{IIb}\beta_3$ [15]. In contrast to PAR-4 deficiency, plasma serotonin levels were similar in ANIT-treated wild-type and Fib$\gamma^{\Delta 5}$ mice (37 ± 4 ng/ml vs. 41 ± 8 ng/ml, respectively, n=6). However, serum ALT activity and bile acids were significantly higher in ANIT-treated Fib$\gamma^{\Delta 5}$mice compared to ANIT-treated wild-type mice (Fig. 5A–B). Serum ALP activity increased in ANIT-treated mice of both genotypes (Fig. 5C). The overall histological appearance of control diet fed wild-type and Fib$\gamma^{\Delta 5}$ mice was similar (Fig. 5D). Extensive multifocal acute hepatocellular coagulative necrosis was present in ANIT-treated Fib$\gamma^{\Delta 5}$ mice, and this was minimal in ANIT-treated wild-type mice (Fig. 5D–E). Although necrotic foci were of similar size in wild-type mice and Fib$\gamma^{\Delta 5}$ mice, the number of necrotic foci and thus, total area of necrosis, were significantly increased in ANIT-treated Fib$\gamma^{\Delta 5}$ mice (Fig. 5F). Potentially owing to expression of tissue factor by injured hepatocytes [31], plasma TAT levels were significantly elevated in ANIT-treated Fib$\gamma^{\Delta 5}$ mice (5.8 ± 0.9 ng/ml, n=6) compared to ANIT-treated wild-type mice (3.5 ± 0.25 ng/ml, n=6). Biliary hyperplasia was also exacerbated in ANIT-treated Fib$\gamma^{\Delta 5}$ mice, as indicated by a significant increase in CK19 staining (Supplemental Fig. 2C–D).

Qualitative assessment of liver histopathology indicated markedly increased portal inflammation in livers of ANIT-treated Fib$\gamma^{\Delta 5}$mice compared to ANIT-treated wild-type mice (Fig. 5D–E). In agreement with this observation, CD3+ lymphocyte accumulation was exacerbated in ANIT-treated Fib$\gamma^{\Delta 5}$ mice compared to ANIT-treated wild-type mice (Fig. 6A–B). Neutrophils were also commonly associated with necrotic lesions in ANIT-treated Fib$\gamma^{\Delta 5}$ mice (Supplemental Fig. 4). In agreement with increased cellular inflammation, plasma levels of IL-6, TNFα, IL-4 and KC/Gro were significantly increased in ANIT-treated Fib$\gamma^{\Delta 5}$ mice (Fig. 6C).

Increased liver fibrosis in ANIT-treated Fib$\gamma^{\Delta 5}$ mice

Compared to wild-type mice fed control diet, hepatic expression of profibrogenic COL1A1, TGFβ2, ITGβ6, and TIMP-1 mRNAs was increased in livers of ANIT-treated wild-type mice for 4 weeks, and induction of each gene was significantly enhanced in ANIT-treated Fib$\gamma^{\Delta 5}$mice (Fig. 7A). Moreover, TGFβ1 mRNA levels increased in livers of ANIT-treated Fib$\gamma^{\Delta 5}$mice (Fig. 7A). Compared to ANIT-treated wild-type mice, α-SMA staining was

dramatically increased near bile ducts in livers of ANIT-treated Fib$\gamma^{\Delta 5}$ mice (Fig. 7B–C). Extensive α-SMA staining was evident within and at the periphery of necrotic lesions in ANIT-treated Fib$\gamma^{\Delta 5}$ mice (Fig. 7B). In agreement with these indicators of a profibrogenic response, hepatic collagen deposition was dramatically increased in livers of ANIT-treated Fib$\gamma^{\Delta 5}$ mice compared to ANIT-treated wild-type mice, as indicated by sirius red staining (Fig. 8A–B) and type 1 collagen immunofluorescence (Fig. 8C–D).

Discussion

The literature is somewhat perplexing as to the role of platelets in liver disease, and it is challenging to conclude that platelets have a unified role in all forms of liver injury and fibrosis. Differences in the experimental basis of liver damage, subtle changes in the timing, duration and/or extent of thrombocytopenia, and the potency/efficacy of antiplatelet interventions (genetic or pharmacologic) may each impact interpretation of the role of platelets. For example, whereas platelet-derived serotonin is reported to promote liver repair/regeneration and inhibit liver fibrosis in some systems [22, 28, 32, 33], its role is reversed in settings of viral hepatitis and non-alcoholic steatohepatitis [34, 35]. Platelets contribute to the acute phase of cholestatic liver injury induced by BDL or a single, large dose of ANIT [19–21]. Likewise, short term (48 hour) antibody-mediated thrombocytopenia reduced hepatic α-SMA levels in 8-week-old Mdr2$^{-/-}$ mice [18]. In contrast, prolonged thrombocytopenia exacerbates long-term BDL-induced liver fibrosis, as does a lack of peripheral serotonin [17, 22]. Notably, a similar dichotomy exists for the role of fibrin(ogen). For example, where fibrin(ogen) is deleterious in acute ANIT hepatotoxicity [36], our findings here in Fib$\gamma^{\Delta 5}$ mice and previously in fibrin(ogen)-null mice [26] suggest that protective properties of fibrin(ogen) emerge as the liver insult becomes chronic. Collectively, these studies highlight the diverse functions of platelets in liver disease, and emphasize a need to obtain a deeper understanding of the context-dependent role of platelets in liver disease.

PAR-1 and $\alpha_{IIB}\beta_3$ antagonists represent targets for antiplatelet therapy in humans [37, 38] and similar effects on platelet activation are observed in PAR-4-deficient mice [12], in $\alpha_{IIB}\beta_3$-deficient mice [39, 40], and in mice expressing $\gamma^{\Delta 5}$ fibrin(ogen) [15], which does not support platelet aggregation. Here, we found that PAR-4 deficiency and disruption of fibrin(ogen) engagement of $\alpha_{IIB}\beta_3$ increased fibrosis caused by chronic biliary injury. In contrast, a recent study found that aspirin significantly reduced fibrosis in Mdr2$^{-/-}$ mice, another model of peribiliary fibrosis [18]. By way of comparison, aspirin prolonged bleeding time by 1.4-fold [18], whereas bleeding times are prolonged by >5-fold in PAR-4$^{-/-}$ mice and Fib$\gamma^{\Delta 5}$ mice [12, 15]. This suggests that severe defects in platelet function (e.g., lack of thrombin signaling or fibrin(ogen) engagement) can result in increased liver fibrosis, analogous to long-term thrombocytopenia. In contrast, less potent inhibition of platelet activation (e.g., aspirin) may inhibit liver fibrosis, yet preserve protective platelet functions.

Several studies have implicated platelet-derived serotonin as a mediator capable of suppressing cholestatic liver injury and biliary fibrosis [22, 33, 41]. However, the mechanism whereby platelets are stimulated to release serotonin during cholestasis has not

been fully characterized. We found that PAR-4 deficiency significantly reduced thrombin-mediated serotonin release in isolated mouse platelets, and plasma serotonin did not increase in ANIT-treated PAR-4$^{-/-}$ mice. This strongly suggests that thrombin-mediated platelet activation is central to serotonin release in cholestasis, although additional studies will be required to elucidate whether changes in serotonin contribute to increased fibrosis in PAR-4$^{-/-}$ mice. Our results are at least consistent with those in the BDL model, where defective platelet serotonin release is associated with alterations in the bile acid pool, a proposed mechanism whereby liver fibrosis is exacerbated [22].

Disruption of thrombin signaling and fibrin-$\alpha_{IIB}\beta_3$ integrin engagement, in PAR-4$^{-/-}$ mice and Fib$\gamma^{\Delta 5}$mice, respectively, increased hepatocyte injury in mice fed ANIT diet, as indicated by serum ALT activity and liver necrosis. However, the severity of hepatocellular necrosis was more dramatic in ANIT-treated Fib$\gamma^{\Delta 5}$mice, and profibrogenic changes such as fibroblast activation and collagen deposition within necrotic areas suggest incomplete repair of necrosis. Whereas changes in plasma serotonin may account for liver pathology in PAR-4$^{-/-}$ mice, plasma serotonin levels in ANIT-treated mice were unaffected by fibrin(ogen) mutation. This suggests that the $\alpha_{IIb}\beta_3$ integrin-fibrin interaction does not augment platelet serotonin release in this context. In other settings, fibrin(ogen) engagement of integrin $\alpha_{IIB}\beta_3$ can facilitate wound repair by promoting platelet aggregation and clot retraction [42, 43]. It is conceivable that in the context of chronic cholestatic liver injury, $\gamma^{\Delta 5}$ fibrin(ogen) fails to support appropriate platelet aggregation and localized release of repair mediators. Additional studies are required to determine whether defective liver repair causes increased liver necrosis in ANIT-treated Fib$\gamma^{\Delta 5}$ mice.

Strong experimental evidence in BDL, carbon tetrachloride and ANIT models indicates that the thrombin receptor PAR-1 contributes to fibrosis in multiple tissues, including the liver [2, 4, 7, 8]. Use of PAR-1$^{-/-}$ mice does not directly address the role of thrombin-mediated platelet activation in liver fibrosis, because platelets in PAR-1 null mice are fully responsive to thrombin [10]. Likewise, PAR-1 activation of stellate cells and portal fibroblasts would be retained in PAR-4 null mice, despite a lack of thrombin signaling in platelets. The observation that PAR-4 deficiency increased liver fibrosis in a model where PAR-1 deficiency reduces fibrosis suggests dichotomous roles of thrombin in this experimental setting. It would be interesting to observe the combined effect of platelet and non-platelet PAR signaling on liver fibrosis. Possible approaches include use of PAR-1/PAR-4 double deficient mice, although the phenotype of these mice has not been described. Alternatively, PAR-4$^{-/-}$ mice administered a PAR-1 antagonist could closely resemble the anticipated effect of a PAR-1 antagonist in patients. Similarly, it would be interesting to evaluate the impact of PAR-4 deficiency in mice expressing $\gamma^{\Delta 5}$ fibrin(ogen), a scenario representing major defects in platelet activation and hemostatic function.

Recent clinical evidence suggests that low-molecular weight heparin delays hepatic decompensation in patients with advanced liver cirrhosis, a majority of which had viral hepatitis [44]. It will be exciting to see whether novel FDA-approved oral anticoagulants (e.g., rivaroxaban, apixaban, dabigatran) that limit thrombin proteolytic activity, are similarly applied as coagulation-directed therapies for liver pathologies. If liver disease (either developing or end-stage) does emerge as an indication for these drugs, it is of

importance to determine how coagulation-mediated platelet activation (ie., through fibrin(ogen) or PARs) participates in other models of liver fibrosis. This is particularly important as elements of hemostasis gain traction as biomarkers and potential therapeutic targets in liver disease.

Supplementary Material

Refer to Web version on PubMed Central for supplementary material.

Acknowledgments

Funding information

This work was supported by the National Institutes of Health National Institute of Environmental Health Sciences [R01 ES017537]. The content is solely the responsibility of the authors and does not necessarily represent the official views of the National Institute of Environmental Health Sciences or the National Institutes of Health.

Abbreviations

ANIT	Alpha-naphthylisothiocyanate
TGF-β	Transforming growth factor beta
ITGB6	Integrin beta 6
$\alpha_{IIb}\beta_3$	alphaIIbbeta3 integrin
αVβ6	alphaVbeta6 integrin
TIMP1	Tissue inhibitor of metalloproteinase1
BDL	Bile duct ligation
BDEC	Bile duct epithelial cell
PAR	Protease activated receptor

References

1. Pihusch R, Rank A, Gohring P, Pihusch M, Hiller E, Beuers U. Platelet function rather than plasmatic coagulation explains hypercoagulable state in cholestatic liver disease. Journal of hepatology. 2002; 37:548–55. [PubMed: 12399218]
2. Sullivan BP, Weinreb PH, Violette SM, Luyendyk JP. The coagulation system contributes to alphaVbeta6 integrin expression and liver fibrosis induced by cholestasis. The American journal of pathology. 2010; 177:2837–49.10.2353/ajpath.2010.100425 [PubMed: 21037076]
3. Ben-Ari Z, Panagou M, Patch D, Bates S, Osman E, Pasi J, Burroughs A. Hypercoagulability in patients with primary biliary cirrhosis and primary sclerosing cholangitis evaluated by thrombelastography. Journal of hepatology. 1997; 26:554–9. [PubMed: 9075662]
4. Fiorucci S, Antonelli E, Distrutti E, Severino B, Fiorentina R, Baldoni M, Caliendo G, Santagada V, Morelli A, Cirino G. PAR1 antagonism protects against experimental liver fibrosis. Role of proteinase receptors in stellate cell activation. Hepatology. 2004; 39:365–75. [PubMed: 14767989]
5. Anstee QM, Dhar A, Thursz MR. The role of hypercoagulability in liver fibrogenesis. Clinics and research in hepatology and gastroenterology. 2011; 35:526–33.10.1016/j.clinre.2011.03.011 [PubMed: 21570930]

6. Tripodi A, Anstee QM, Sogaard KK, Primignani M, Valla DC. Hypercoagulability in cirrhosis: causes and consequences. Journal of thrombosis and haemostasis: JTH. 2011; 9:1713–23.10.1111/j.1538-7836.2011.04429.x [PubMed: 21729237]
7. Rullier A, Gillibert-Duplantier J, Costet P, Cubel G, Haurie V, Petibois C, Taras D, Dugot-Senant N, Deleris G, Bioulac-Sage P, Rosenbaum J. Protease-activated receptor 1 knockout reduces experimentally induced liver fibrosis. American journal of physiology Gastrointestinal and liver physiology. 2008; 294:G226–35.10.1152/ajpgi.00444.2007 [PubMed: 17962354]
8. Kallis YN, Scotton CJ, Mackinnon AC, Goldin RD, Wright NA, Iredale JP, Chambers RC, Forbes SJ. Proteinase activated receptor 1 mediated fibrosis in a mouse model of liver injury: a role for bone marrow derived macrophages. PloS one. 2014; 9:e86241.10.1371/journal.pone.0086241 [PubMed: 24475094]
9. Gaca MD, Zhou X, Benyon RC. Regulation of hepatic stellate cell proliferation and collagen synthesis by proteinase-activated receptors. JHepatol. 2002; 36:362–9. [PubMed: 11867180]
10. Connolly AJ, Ishihara H, Kahn ML, Farese RV Jr, Coughlin SR. Role of the thrombin receptor in development and evidence for a second receptor. Nature. 1996; 381:516–9.10.1038/381516a0 [PubMed: 8632823]
11. Kahn ML, Zheng YW, Huang W, Bigornia V, Zeng D, Moff S, Farese RV Jr, Tam C, Coughlin SR. A dual thrombin receptor system for platelet activation. Nature. 1998; 394:690–4.10.1038/29325 [PubMed: 9716134]
12. Hamilton JR, Cornelissen I, Coughlin SR. Impaired hemostasis and protection against thrombosis in protease-activated receptor 4-deficient mice is due to lack of thrombin signaling in platelets. Journal of thrombosis and haemostasis: JTH. 2004; 2:1429–35.10.1111/j.1538-7836.2004.00783.x [PubMed: 15304051]
13. Gear AR, Burke D. Thrombin-induced secretion of serotonin from platelets can occur in seconds. Blood. 1982; 60:1231–4. [PubMed: 7126874]
14. Bennett JS, Berger BW, Billings PC. The structure and function of platelet integrins. Journal of thrombosis and haemostasis: JTH. 2009; 7 (Suppl 1):200–5.10.1111/j.1538-7836.2009.03378.x [PubMed: 19630800]
15. Holmback K, Danton MJ, Suh TT, Daugherty CC, Degen JL. Impaired platelet aggregation and sustained bleeding in mice lacking the fibrinogen motif bound by integrin alpha IIb beta 3. The EMBO journal. 1996; 15:5760–71. [PubMed: 8918453]
16. Lisman T, Porte RJ. The role of platelets in liver inflammation and regeneration. Seminars in thrombosis and hemostasis. 2010; 36:170–4.10.1055/s-0030-1251501 [PubMed: 20414832]
17. Kodama T, Takehara T, Hikita H, Shimizu S, Li W, Miyagi T, Hosui A, Tatsumi T, Ishida H, Tadokoro S, Ido A, Tsubouchi H, Hayashi N. Thrombocytopenia exacerbates cholestasis-induced liver fibrosis in mice. Gastroenterology. 2010; 138:2487–98. 98 e1–7.10.1053/j.gastro.2010.02.054 [PubMed: 20206174]
18. Yoshida S, Ikenaga N, Liu SB, Peng ZW, Chung J, Sverdlov DY, Miyamoto M, Kim YO, Ogawa S, Arch RH, Schuppan D, Popov Y. Extra-hepatic PDGFB, Delivered by Platelets, Promotes Activation of Hepatic Stellate Cells and Biliary Fibrosis in Mice. Gastroenterology. 201410.1053/j.gastro.2014.08.038
19. Laschke MW, Dold S, Menger MD, Jeppsson B, Thorlacius H. Platelet-dependent accumulation of leukocytes in sinusoids mediates hepatocellular damage in bile duct ligation-induced cholestasis. British journal of pharmacology. 2008; 153:148–56.10.1038/sj.bjp.0707578 [PubMed: 18026126]
20. Sullivan BP, Wang R, Tawfik O, Luyendyk JP. Protective and damaging effects of platelets in acute cholestatic liver injury revealed by depletion and inhibition strategies. Toxicological sciences: an official journal of the Society of Toxicology. 2010; 115:286–94.10.1093/toxsci/kfq042 [PubMed: 20133375]
21. Bailie MB, Pearson JM, Lappin PB, Killam AL, Roth RA. Platelets and alpha-naphthylisothiocyanate-induced liver injury. Toxicology and applied pharmacology. 1994; 129:207–13.10.1006/taap.1994.1245 [PubMed: 7992311]
22. Jang JH, Rickenbacher A, Humar B, Weber A, Raptis DA, Lehmann K, Stieger B, Moritz W, Soll C, Georgiev P, Fischer D, Laczko E, Graf R, Clavien PA. Serotonin protects mouse liver from

cholestatic injury by decreasing bile salt pool after bile duct ligation. Hepatology. 2012; 56:209–18.10.1002/hep.25626 [PubMed: 22290718]

23. Lisman T, Weeterings C, de Groot PG. Platelet aggregation: involvement of thrombin and fibrin(ogen). Frontiers in bioscience: a journal and virtual library. 2005; 10:2504–17. [PubMed: 15970513]
24. Sambrano GR, Weiss EJ, Zheng YW, Huang W, Coughlin SR. Role of thrombin signalling in platelets in haemostasis and thrombosis. Nature. 2001; 413:74–8.10.1038/35092573 [PubMed: 11544528]
25. Kassel KM, Sullivan BP, Cui W, Copple BL, Luyendyk JP. Therapeutic administration of the direct thrombin inhibitor argatroban reduces hepatic inflammation in mice with established fatty liver disease. The American journal of pathology. 2012; 181:1287–95.10.1016/j.ajpath.2012.06.011 [PubMed: 22841818]
26. Luyendyk JP, Kassel KM, Allen K, Guo GL, Li G, Cantor GH, Copple BL. Fibrinogen deficiency increases liver injury and early growth response-1 (Egr-1) expression in a model of chronic xenobiotic-induced cholestasis. The American journal of pathology. 2011; 178:1117–25.10.1016/j.ajpath.2010.11.064 [PubMed: 21356363]
27. Vandesompele J, De Preter K, Pattyn F, Poppe B, Van Roy N, De Paepe A, Speleman F. Accurate normalization of real-time quantitative RT-PCR data by geometric averaging of multiple internal control genes. Genome biology. 2002; 3:RESEARCH0034. [PubMed: 12184808]
28. Starlinger P, Assinger A, Haegele S, Wanek D, Zikeli S, Schauer D, Birner P, Fleischmann E, Gruenberger B, Brostjan C, Gruenberger T. Evidence for serotonin as a relevant inducer of liver regeneration after liver resection in humans. Hepatology. 2014; 60:257–66.10.1002/hep.26950 [PubMed: 24277679]
29. Donahower B, McCullough SS, Kurten R, Lamps LW, Simpson P, Hinson JA, James LP. Vascular endothelial growth factor and hepatocyte regeneration in acetaminophen toxicity. American journal of physiology Gastrointestinal and liver physiology. 2006; 291:G102–9.10.1152/ajpgi.00575.2005 [PubMed: 16565415]
30. Thurman JM, Holers VM. The central role of the alternative complement pathway in human disease. J Immunol. 2006; 176:1305–10. [PubMed: 16424154]
31. Sullivan BP, Kopec AK, Joshi N, Cline H, Brown JA, Bishop SC, Kassel KM, Rockwell C, Mackman N, Luyendyk JP. Hepatocyte tissue factor activates the coagulation cascade in mice. Blood. 2013; 121:1868–74.10.1182/blood-2012-09-455436 [PubMed: 23305736]
32. Ebrahimkhani MR, Oakley F, Murphy LB, Mann J, Moles A, Perugorria MJ, Ellis E, Lakey AF, Burt AD, Douglass A, Wright MC, White SA, Jaffre F, Maroteaux L, Mann DA. Stimulating healthy tissue regeneration by targeting the 5-HT(2)B receptor in chronic liver disease. Nature medicine. 2011; 17:1668–73.10.1038/nm.2490
33. Lesurtel M, Graf R, Aleil B, Walther DJ, Tian Y, Jochum W, Gachet C, Bader M, Clavien PA. Platelet-derived serotonin mediates liver regeneration. Science. 2006; 312:104–7.10.1126/science.1123842 [PubMed: 16601191]
34. Lang PA, Contaldo C, Georgiev P, El-Badry AM, Recher M, Kurrer M, Cervantes-Barragan L, Ludewig B, Calzascia T, Bolinger B, Merkler D, Odermatt B, Bader M, Graf R, Clavien PA, Hegazy AN, Lohning M, Harris NL, Ohashi PS, Hengartner H, Zinkernagel RM, Lang KS. Aggravation of viral hepatitis by platelet-derived serotonin. Nature medicine. 2008; 14:756–61.10.1038/nm1780
35. Nocito A, Dahm F, Jochum W, Jang JH, Georgiev P, Bader M, Renner EL, Clavien PA. Serotonin mediates oxidative stress and mitochondrial toxicity in a murine model of nonalcoholic steatohepatitis. Gastroenterology. 2007; 133:608–18.10.1053/j.gastro.2007.05.019 [PubMed: 17681180]
36. Luyendyk JP, Mackman N, Sullivan BP. Role of fibrinogen and protease-activated receptors in acute xenobiotic-induced cholestatic liver injury. Toxicological sciences: an official journal of the Society of Toxicology. 2011; 119:233–43.10.1093/toxsci/kfq327 [PubMed: 20974703]
37. Tricoci P, Huang Z, Held C, Moliterno DJ, Armstrong PW, Van de Werf F, White HD, Aylward PE, Wallentin L, Chen E, Lokhnygina Y, Pei J, Leonardi S, Rorick TL, Kilian AM, Jennings LH, Ambrosio G, Bode C, Cequier A, Cornel JH, Diaz R, Erkan A, Huber K, Hudson MP, Jiang L, Jukema JW, Lewis BS, Lincoff AM, Montalescot G, Nicolau JC, Ogawa H, Pfisterer M, Prieto JC,

Ruzyllo W, Sinnaeve PR, Storey RF, Valgimigli M, Whellan DJ, Widimsky P, Strony J, Harrington RA, Mahaffey KW, Investigators T. Thrombin-receptor antagonist vorapaxar in acute coronary syndromes. The New England journal of medicine. 2012; 366:20–33.10.1056/NEJMoa1109719 [PubMed: 22077816]

38. Bledzka K, Smyth SS, Plow EF. Integrin alphaIIbbeta3: from discovery to efficacious therapeutic target. Circulation research. 2013; 112:1189–200.10.1161/CIRCRESAHA.112.300570 [PubMed: 23580774]
39. Tronik-Le Roux D, Roullot V, Poujol C, Kortulewski T, Nurden P, Marguerie G. Thrombasthenic mice generated by replacement of the integrin alpha(IIb) gene: demonstration that transcriptional activation of this megakaryocytic locus precedes lineage commitment. Blood. 2000; 96:1399–408. [PubMed: 10942384]
40. Hodivala-Dilke KM, McHugh KP, Tsakiris DA, Rayburn H, Crowley D, Ullman-Cullere M, Ross FP, Coller BS, Teitelbaum S, Hynes RO. Beta3-integrin-deficient mice are a model for Glanzmann thrombasthenia showing placental defects and reduced survival. J Clin Invest. 1999; 103:229–38.10.1172/JCI5487 [PubMed: 9916135]
41. Lieu HT, Batteux F, Simon MT, Cortes A, Nicco C, Zavala F, Pauloin A, Tralhao JG, Soubrane O, Weill B, Brechot C, Christa L. HIP/PAP accelerates liver regeneration and protects against acetaminophen injury in mice. Hepatology. 2005; 42:618–26.10.1002/hep.20845 [PubMed: 16116631]
42. Gawaz M, Vogel S. Platelets in tissue repair: control of apoptosis and interactions with regenerative cells. Blood. 2013; 122:2550–4.10.1182/blood-2013-05-468694 [PubMed: 23963043]
43. Laurens N, Koolwijk P, de Maat MP. Fibrin structure and wound healing. Journal of thrombosis and haemostasis: JTH. 2006; 4:932–9.10.1111/j.1538-7836.2006.01861.x [PubMed: 16689737]
44. Villa E, Camma C, Marietta M, Luongo M, Critelli R, Colopi S, Tata C, Zecchini R, Gitto S, Petta S, Lei B, Bernabucci V, Vukotic R, De Maria N, Schepis F, Karampatou A, Caporali C, Simoni L, Del Buono M, Zambotto B, Turola E, Fornaciari G, Schianchi S, Ferrari A, Valla D. Enoxaparin prevents portal vein thrombosis and liver decompensation in patients with advanced cirrhosis. Gastroenterology. 2012; 143:1253–60. e1–4.10.1053/j.gastro.2012.07.018 [PubMed: 22819864]

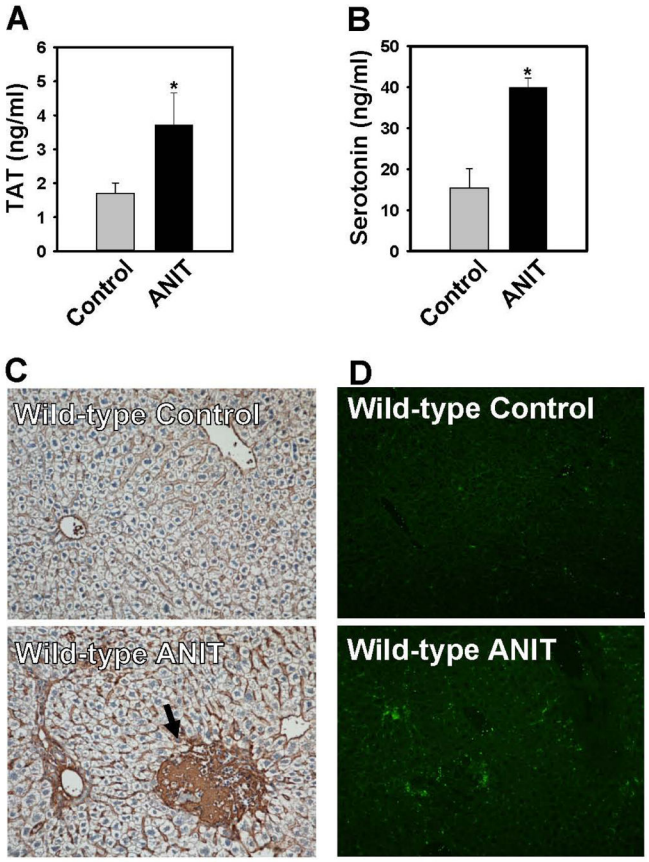

Figure 1. Coagulation and hepatic platelet accumulation in ANIT-treated wild-type mice

Wild-type mice were fed control diet (AIN-93M) or an identical diet containing 0.025% ANIT for 4 weeks. (A) Plasma TAT levels were determined by ELISA. (B) Plasma serotonin levels were determined by ELISA. (C) Representative photomicrographs (200X) showing liver sections stained for fibrin(ogen) (brown). Arrow indicates area of acute hepatocellular coagulative necrosis. (D) Representative photomicrographs (100X) show liver sections stained for integrin α_{IIb} (CD41, platelets). Data are expressed as mean ± SEM, n = 5 mice per group for control diet and 10 mice per group for ANIT-treated mice, *$p<0.05$ vs. control diet.

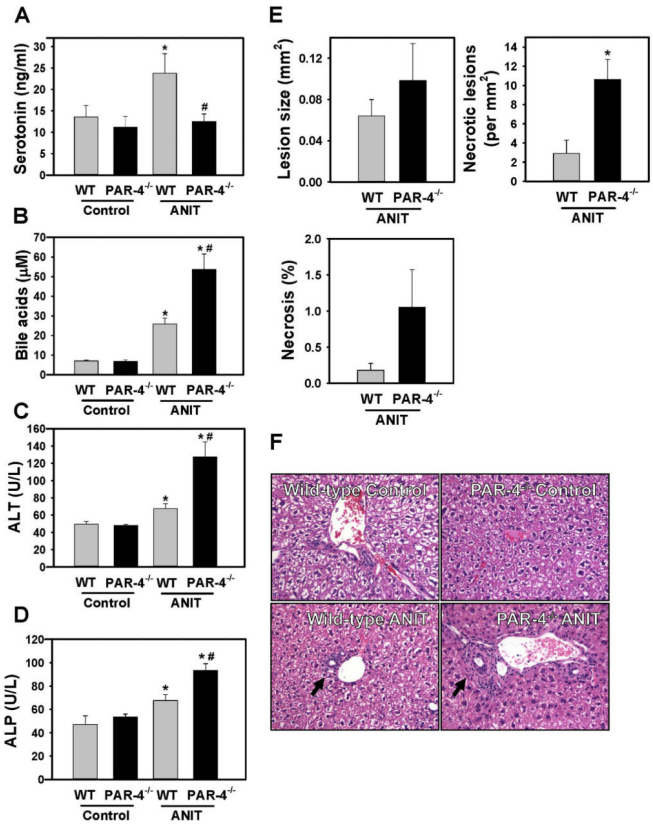

Figure 2. Effect of PAR-4 deficiency on serotonin levels and liver injury in ANIT-treated mice

Wild-type (WT) and PAR-4$^{-/-}$ mice were fed control diet (AIN-93M) or an identical diet containing 0.025% ANIT for 4 weeks. (A) Plasma serotonin, (B) serum bile acids, (C) serum ALT activity and (D) serum ALP activity were determined as described in Materials and Methods. (E) Necrotic lesion size, number and area were determined as described in Materials and Methods. (F) Representative photomicrographs showing hematoxylin and eosin–stained liver sections (200X). Arrow indicates area of biliary fibrosis and portal inflammation. Data are expressed as mean ± SEM; n = 5 mice per group for control diet and 10–11 mice per group for ANIT-treated mice. *p<0.05 vs. control diet within genotype and #p<0.05 vs. WT mice fed the same diet.

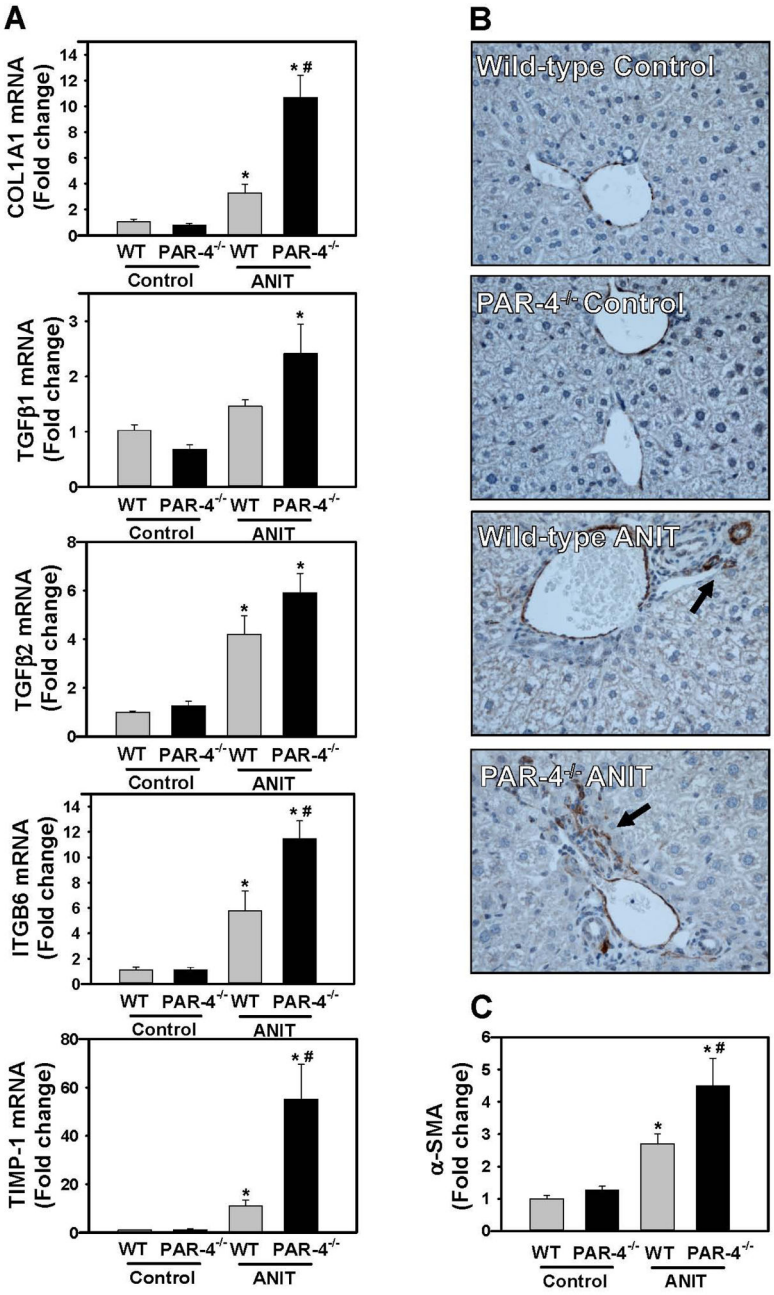

Figure 3. Increased profibrogenic gene expression in livers of ANIT-treated PAR-4$^{-/-}$ mice

Wild-type (WT) and PAR-4$^{-/-}$ mice were fed control diet (AIN-93M) or an identical diet containing 0.025% ANIT for 4 weeks. (A) Hepatic expression of mRNAs encoding COL1A1, TGFβ1, TGFβ2, ITGβ6 and TIMP-1 was determined by real-time qPCR. (B) Representative photomicrographs (200X) show liver sections stained for α-smooth muscle actin (α-SMA) (brown). Arrow indicates peribiliary α-SMA staining. (C) α-SMA was quantified as described in Materials and Methods and expressed as fold change. Data are expressed as mean ± SEM; n = 5 mice per group for control diet and 10–11 mice per group

for mice fed ANIT diet. *$p<0.05$ vs. control diet within genotype and #$p<0.05$ vs. wild-type mice fed the same diet.

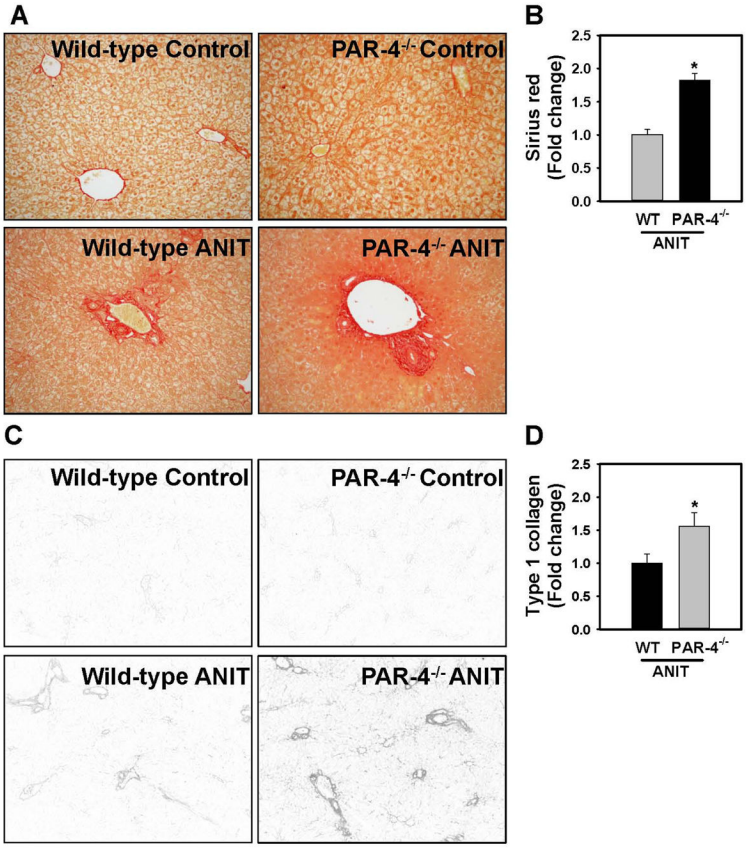

Figure 4. Increased collagen deposition in livers of ANIT-treated PAR-4$^{-/-}$ mice

Wild-type (WT) and PAR-4$^{-/-}$ mice were fed control diet (AIN-93M) or an identical diet containing 0.025% ANIT for 4 weeks. Representative photomicrographs showing liver sections stained with (A) sirius red staining (200X) and (C) immunofluorescent type 1 collagen staining (100X), converted to grayscale and inverted such that type 1 collagen staining is dark. (B) Sirius red staining and (D) Type 1 collagen staining was quantified as described in Materials and Methods. Data are expressed as mean ± SEM; n = 5 mice per group for control diet and 10–11 mice per group for mice fed ANIT diet. *p<0.05 vs. ANIT-treated WT mice.

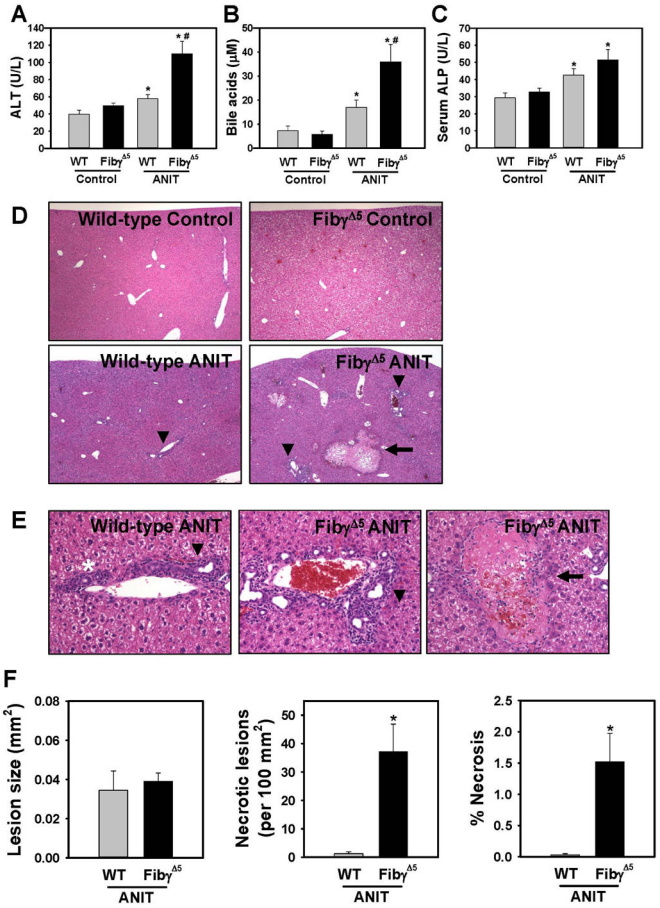

Figure 5. Increased hepatocellular necrosis in ANIT-treated Fibγ^{Δ5} mice

Wild-type (WT) and Fibγ^{Δ5}mice were fed control diet (AIN-93M) or an identical diet containing 0.025% ANIT for 4 weeks. (A) Serum ALT activity, (B) serum bile acid concentration, and (C) serum ALP activity were determined as described in Materials and Methods. Representative photomicrographs show hematoxylin and eosin–stained liver sections at (D) low magnification (40X) and (E) high magnification (200X). Arrows indicate area of hepatocellular coagulative necrosis. Arrowheads indicate area of biliary fibrosis and portal inflammation. (F) Necrotic lesion size, number and area were determined as described in Materials and Methods. Data are expressed as mean ± SEM; n = 4 mice per group for control diet and 9–10 mice per group for mice fed ANIT diet. *p<0.05 vs. control diet within genotype and #p<0.05 vs. WT mice fed the same diet.

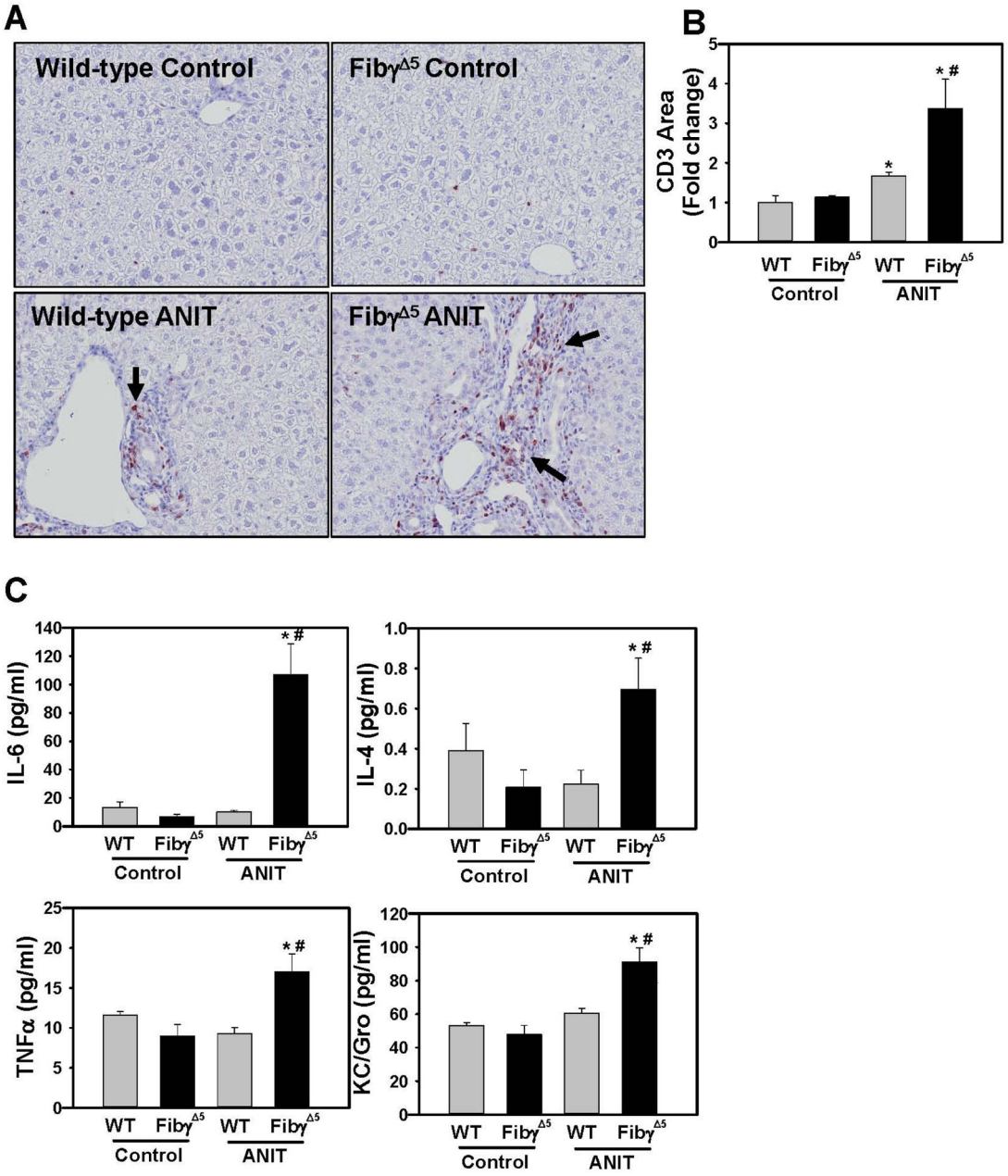

Figure 6. Increased hepatic inflammation in ANIT-treated Fibγ^{Δ5} mice

Wild-type (WT) and Fibγ^{Δ5} mice were fed control diet (AIN-93M) or an identical diet containing 0.025% ANIT for 4 weeks. (A) Representative photomicrographs (200X) and (B) quantification of CD3 staining. (C) Serum levels of cytokines IL-6, IL-4, KC/Gro, and TNFα were determined as described in Materials and Methods. Data are expressed as mean ± SEM; n = 4 mice per group for control diet and 9–10 mice per group for mice fed ANIT diet. *p<0.05 vs. control diet within genotype and #p<0.05 vs. WT mice fed the same diet.

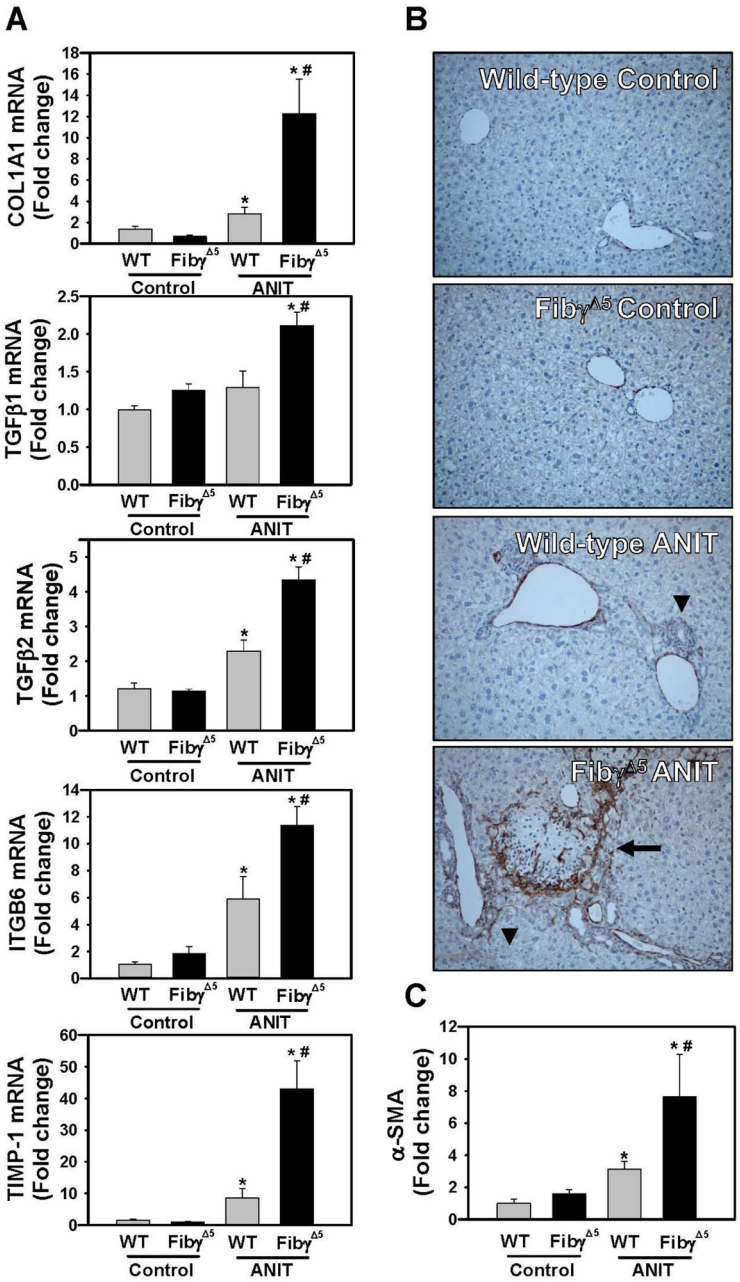

Figure 7. Increased profibrogenic gene induction in livers of ANIT-treated Fibγ$^{\Delta 5}$ mice

Wild-type (WT) and Fibγ$^{\Delta 5}$ mice were fed control diet (AIN-93M) or an identical diet containing 0.025% ANIT for 4 weeks. (A) Hepatic expression of mRNAs encoding the profibrogenic genes COL1A1, TGFβ1, TGFβ2, ITGβ6 and TIMP-1 was determined by real-time qPCR. (B) Representative photomicrographs (200X) show liver sections stained for α-smooth muscle actin (α-SMA) (brown). Arrow heads indicates area of periportal α-SMA staining. Arrow indicates area of α-SMA staining within an area of hepatocellular coagulative necrosis. (C) α-SMA was quantified as described in Materials and Methods and expressed as fold-change. Data are expressed as mean ± SEM; n = 4 mice per group for

control diet and 9–10 mice per group for mice fed ANIT diet. *p<0.05 vs. control diet within genotype and #p<0.05 vs. WT mice fed the same diet.

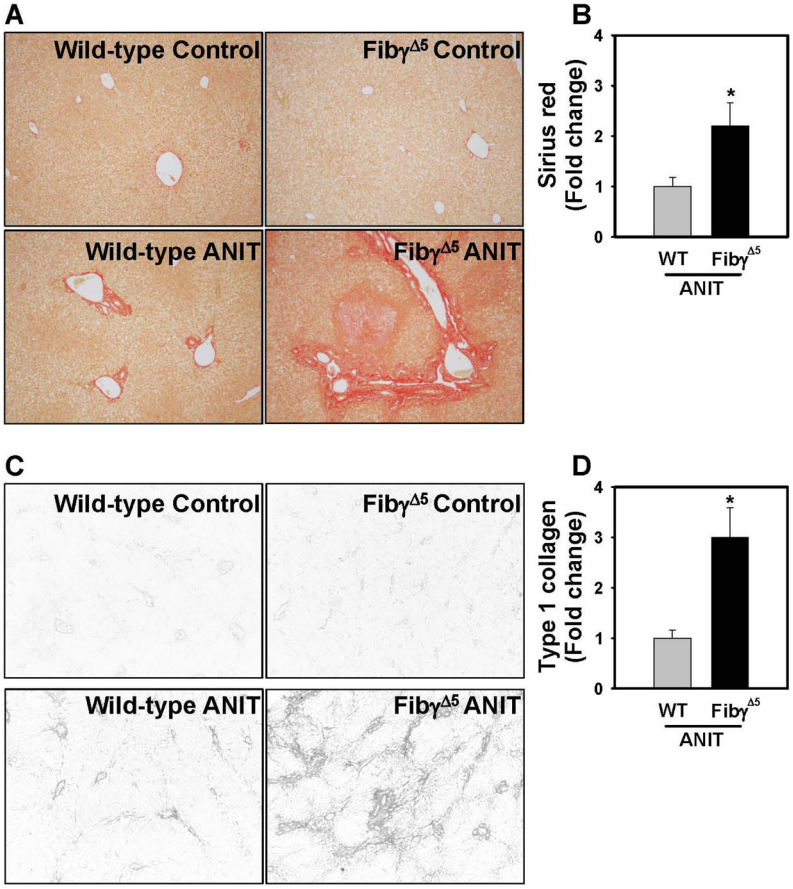

Figure 8. Increased collagen deposition in livers of ANIT-treated Fibγ$^{\Delta 5}$ mice

Wild-type (WT) and Fibγ$^{\Delta 5}$mice were fed control diet (AIN-93M) or an identical diet containing 0.025% ANIT for 4 weeks. Representative photomicrographs showing liver sections stained for (A) Sirius red (200X) and (B) immunofluorescent type 1 collagen (100X). Fluorescent images were converted to grayscale and inverted such that type 1 collagen staining is dark. (C) Sirius red and (D) Type 1 collagen stains were quantified as described in Materials and Methods. Data are expressed as mean ± SEM; n = 4 mice per group for control diet and 9–10 mice per group for mice fed ANIT diet. *$p<0.05$ vs. ANIT-treated WT mice.